Dynamical chiral symmetry with an infrared finite gluon propagator

Journal of Physics: Conference Series **706** (2016) 052018 doi:10.1088/1742-6596/706/5/052018

Dynamical chiral symmetry with an infrared finite gluon propagator

J. C. Cardona and A. C. Aguilar

University of Campinas - UNICAMP, Institute of Physics "Gleb Wataghin", 13083-859 Campinas, SP, Brazil

E-mail: jeinerc@ifi.unicamp.br

Abstract.

In this work we study dynamical quark mass generation using an infrared finite gluon propagator obtained from quenched lattice simulations. The quark gap equation is solved using a purely non-Abelian Ansatz for the quark-gluon vertex, which displays a dependence on the ghost dressing function and the scalar component of quark-ghost scattering kernel. For the former quantity we use quenched lattice results, while for the latter we derive its own integral equation at the one-loop-dressed approximation. This latter quantity is then coupled to the system of equations governing the two Dirac structures of the quark propagator. It turns out that when a current quark mass of 5 MeV is introduced, the constituent quark mass generated from the gap equation is of the order of 310 MeV. In addition, the pion decay constant computed from the resulting quark propagator is in good agreement with the physical value.

1. Introduction

One of the major challenges of the strong interactions is to understand the underlying mechanism that generates masses for the quarks and triggers the subsequent breaking of the chiral symmetry (CS) [1, 2]. It is well known that QCD must be endowed with a very efficient mass generation mechanism, given that the Higgs mechanism accounts for the generation of only 2% of the total mass of the light quarks; thus, the remaining 98% must be accounted for by the internal QCD dynamics [2, 3, 4].

The CS breaking is an inherently nonperturbative phenomenon, whose study in the continuum leads almost invariably to a treatment based on the Schwinger-Dyson equation (SDE) for the quark propagator (gap equation) [1, 5, 6, 7].

Besides the quark propagator, the kernel of this nonlinear integral equation is expressed in terms of three others Green's functions, namely (i) the full gluon propagator, (ii) the full ghost propagator and, (iii) the complete quark-gluon vertex; evidently, each one of these Green's functions satisfies its own SDE. One of the characteristic features of the gap equation is that, in order to give rise to nontrivial solutions, the support of its kernel in the region of few hundred MeV must overcome a critical amount. Within this context, the nonperturbative quark-gluon vertex plays a crucial role in providing the required enhancement at the correct momentum scale [6].

Despite its physical importance, the nonperturbative behavior of this special vertex is still only partially known, mainly due to a variety of serious technical difficulties. In particular,

its rich tensorial structure (composed by 4 longitudinal and 8 transverse structures) leads to the determination of twelve independent form factors, which depend on three kinematic variables [8, 9]. In addition, this vertex controls the way that the ghost sector enters into the gap equation, and introduces a pivotal dependence on the ghost dressing function and the quark-ghost scattering amplitude. This important quantity satisfies its own dynamical equation, which was studied in Ref. [6] under certain simplifying approximations.

In Ref. [6] an approximate version of the gap equation was studied in the chiral limit, using the gluon and the ghost propagators obtained from the quenched lattice simulations [10, 11, 12]. Here we will follow the same steps presented in the Ref. [6] to study the case where the CS is already explicitly broken by the presence of a current quark mass. In addition, we present an integral equation that furnishes an improved one-loop dressed approximation for the scalar component of the quark-ghost scattering kernel.

These proceedings are organized as follows. In Section 2 we introduce the main ingredients and the crucial relations necessary for the study of the CS breaking. In Section 3, we present the structure of the quark-gluon vertex entering into the definition of the gap equation, and derive the dynamical equation for the scalar component of the quark-ghost scattering kernel. In Section 4 the numerical results for the quark dynamical mass are presented and the corresponding value for the pion decay constant is computed from them. Finally, in Section 5 we summarize our conclusions.

2. Basics equations and conventions

In this section we introduce the basic definitions and ingredients used throughout this work. Let us start with the definition of the full gluon propagator, that in Landau gauge, takes the form

$$i\Delta_{\mu\nu}(q) = -i\left[g_{\mu\nu} - \frac{q_\mu q_\nu}{q^2}\right]\Delta(q^2)\,. \tag{1}$$

In addition, it is usual to decompose the quark propagator, $S(p)$, in terms of a Dirac vector component $A(p^2)$, and a scalar component $B(p^2)$ in the following way [1, 6]

$$S^{-1}(p) = A(p^2)\not{p} - B(p^2) - m_0 = A(p^2)[\not{p} - \mathcal{M}(p^2)] - m_0\,. \tag{2}$$

where we have defined the dynamical quark mass function as $\mathcal{M}(p^2) = B(p^2)/A(p^2)$. Notice that when $m_0 \neq 0$ the chiral symmetry is explicitly broken by the presence of a current quark mass. Moreover, the dynamical breaking only occurs when the scalar function $B(p^2)$ acquires a nonvanishing value.

In Fig. 1 we show the diagrammatic representation of the quark SDE. The gray circles represent the complete quark and gluon propagators and the full quark-gluon vertex.

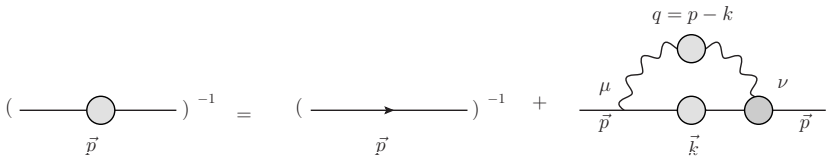

Figure 1. The quark SDE, given by Eq. (3). The grey blobs represent the full gluon and quark propagators and the complete quark-gluon vertex.

Following the momentum convention and the Lorentz indices indicated in Fig. 1, the renormalized SDE for the quark propagator is written as

$$S^{-1}(p) = Z_F(\not{p} - m_0) - Z_1 C_{\rm F} g^2 \int_k \gamma_\mu S(k)\Gamma_\nu(-p,k,q)\Delta^{\mu\nu}(q)\,, \tag{3}$$

where Γ_ν is the full quark-gluon vertex, $Z_1(\mu)$ and $Z_F(\mu)$ are the vertex and the quark wave-function renormalization constants, respectively. Here m_0 is the current bare mass and $C_{\rm F}$ is the Casimir eigenvalue for the fundamental representation. In addition, we have introduced the shorthand notation $\int_k \equiv (2\pi)^{-4}\int d^4k$.

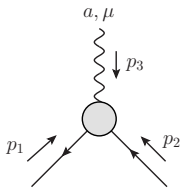

Figure 2. The full quark-gluon vertex.

An essential ingredient in the above equation is the full quark-gluon vertex, illustrated in Fig. 2, and written as

$$\Gamma^a_\mu(p_1,p_2,p_3) = gt^a\Gamma_\mu(p_1,p_2,p_3)\,,$$

where all momenta p_i are entering as showed in Fig. 2, and $t^a = \lambda^a/2$, where λ^a are the Gell-Mann matrices.

The vertex Γ_μ satisfies the fundamental Slavnov-Taylor identity (STI) [13]

$$q^\mu\Gamma_\mu(p_1,p_2,q) = F(q)[S^{-1}(-p_1)H(p_1,p_2,q) - \overline{H}(p_2,p_1,q)S^{-1}(p_2)]\,, \tag{4}$$

where $H(p_1,p_2,q)$ is the quark-ghost scattering amplitude represented in Fig. 3, and $F(q^2)$ is the dressing of the full ghost propagator, defined as

$$D(q^2) = \frac{F(q^2)}{q^2}. \tag{5}$$

The quark-ghost scattering amplitude $H(p_1,p_2,q)$ and its "conjugate" $\overline{H}(p_1,p_2,q)$ has the following Lorentz decomposition [6, 14]

$$\begin{aligned} H(p_1,p_2,q) &= X_0\,\mathbb{I} + X_1\not{p}_1 + X_2\not{p}_2 + X_3\,\tilde{\sigma}_{\mu\nu}p_1^\mu p_2^\nu\,,\\ \overline{H}(p_2,p_1,q) &= \overline{X}_0\,\mathbb{I} - \overline{X}_2\not{p}_1 - \overline{X}_1\not{p}_2 + \overline{X}_3\,\tilde{\sigma}_{\mu\nu}p_1^\mu p_2^\nu\,, \end{aligned} \tag{6}$$

where the form factors X_i are functions of the momenta, $X_i = X_i(p_1,p_2,q)$, $\overline{X}_i = \overline{X}_i(p_2,p_1,q)$, and $\tilde{\sigma}_{\mu\nu} \equiv \frac{1}{2}[\gamma_\mu,\gamma_\nu]$.

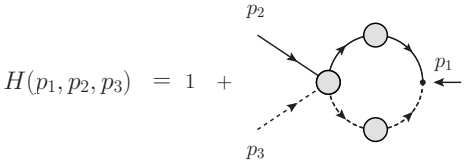

Figure 3. The quark-ghost scattering kernel $H(p_1,p_2,p_3)$.

Thus, we clearly see from Eqs (3) and (4) that most of the dynamics of the ghost sector will be introduced into the kernel of the gap equation by means of the full quark-gluon vertex.

It is interesting to notice that the STI, given by Eq. (4), enforces the all-older constraint [6]

$$Z_1 = Z_c^{-1} Z_F Z_H^{-1}, \tag{7}$$

where Z_c and Z_H are the renormalization constants of the ghost propagator and the quark-ghost scattering kernel, respectively. In the next section, these constants we will be fixed using the momentum subtraction scheme (MOM). Specifically, in this scheme the renormalized propagators and vertices should satisfy

$$\begin{aligned} F(q^2)|_{q^2=\mu^2} &= 1\,, \qquad S^{-1}(p)|_{p^2=\mu^2} = \not{p} - m(\mu)\,, \\ \Delta^{-1}(q^2)|_{q^2=\mu^2} &= \mu^2\,, \qquad \Gamma_\mu(p_1,p_2,q)|_{p_1^2=p_2^2=q^2=\mu^2} = \gamma_\mu\,, \\ H(p_1,p_2,q)|_{p_1^2=p_2^2=q^2=\mu^2} &= 1\,, \end{aligned} \tag{8}$$

where μ is renormalization (subtraction) point.

3. The quark-gluon vertex and the gap equation

Let us now turn our attention to the quark-gluon vertex. This vertex can be separated into longitudinal and transverse parts in the following way [8, 9]

$$\Gamma_\mu(p_1,p_2,q) = \Gamma^L_\mu(p_1,p_2,q) + \Gamma^T_\mu(p_1,p_2,p_3)\,, \tag{9}$$

where the transversal part $\Gamma^T_\mu(p_1,p_2,q)$ satisfies automatically the STI of Eq. (4), since $q^\mu\Gamma^T_\mu(p_1,p_2,q) = 0$.

The most general Lorentz decomposition for the longitudinal part of the vertex $\Gamma^L_\mu(p_1,p_2,q)$ can be written as [14]

$$\Gamma^L_\mu = L_1\gamma_\mu + L_2(\not{p}_1 - \not{p}_2)(p_1-p_2)_\mu + L_3(p_1-p_2)_\mu + L_4\tilde{\sigma}_{\mu\nu}(p_1-p_2)^\nu\,, \tag{10}$$

where $L_i = L_i(p_1,p_2,q)$ are the form factors, whose dependence on the momenta has been suppressed to keep a compact notation. Notice that the tree level expression is recovered by setting $L_1 = 1$ and $L_2 = L_3 = L_4 = 0$; then, $\Gamma^{[0]}_\mu = \gamma_\mu$.

Due to the fact that the behavior of the vertex Γ^L_μ is constrained by the STI of Eq. (4), the form factors L_i's appearing in the Eq. (10) are given in terms of the form factors X_is of Eq. (6). The full expressions for L_i's in terms of the form factors X_is can be found in Ref. [6]. Here, for the sake of simplicity, we will consider the case where only the scalar component of the quark-ghost scattering kernel is non-vanishing *i.e.* $X_0 \neq 0$ while $X_i = \overline{X}_i = 0$ for $i \geq 1$. In this limit, we obtain that

$$\begin{aligned} L_1 &= F(q)X_0(q)\left[\frac{A(p_1)+A(p_2)}{2}\right] \\ L_2 &= F(q)X_0(q)\left[\frac{A(p_1)-A(p_2)}{2(p_1^2-p_2^2)}\right] \\ L_3 &= F(q)X_0(q)\left[\frac{B(p_1)-B(p_2)}{(p_1^2-p_2^2)}\right] \\ L_4 &= 0 \end{aligned} \tag{11}$$

According the above expression, the form factors L_i display an explicit dependence on the product $F(q)X_0(q)$, thus carrying valuable information about the ghost infrared sector of the

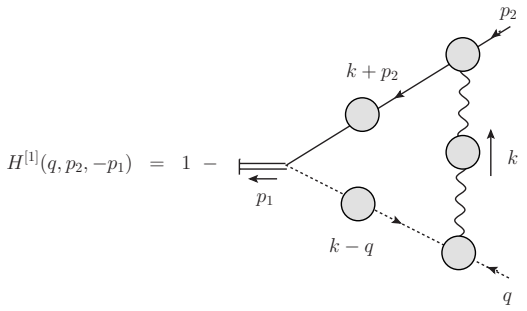

Figure 4. The quark-ghost scattering kernel at "one-loop dressed" approximation.

theory. It is interesting to notice that in the limit of $F(q)X_0(q) = 1$, the form factors of Eq. (11) reduce to the so-called Ball-Chiu (BC) vertex, Γ^{BC}_μ [15]. Therefore, our final Ansatz for the longitudinal part of the vertex is given by

$$\Gamma^L_\mu(p_1, p_2, q) = F(q)X_0(q)\Gamma^{BC}_\mu(p_1, p_2, q)\,, \tag{12}$$

Substituting the vertex Γ^L_μ defined in the Eqs. (10) and (11) into the gap equation (3), we arrive at the following coupled system for $A(p)$ and $B(p)$

$$\begin{aligned} A(p) &= Z_F + Z_c^{-1} g^2 C_{\rm F} \int_k \frac{\Delta(q)F(q)X_0(q)}{A^2(k)k^2 + B^2(k)} \mathcal{K}_A(p,k)\,, \\ B(p) &= Z_4 m + Z_c^{-1} g^2 C_{\rm F} \int_k \frac{\Delta(q)F(q)X_0(q)}{A^2(k)k^2 + B^2(k)} \mathcal{K}_B(p,k)\,, \end{aligned} \tag{13}$$

where $q = p - k$, $\mathcal{K}_A(p,k)$ and $\mathcal{K}_B(p,k)$ are kernels defined in Ref. [6].

In order to proceed further, now we derive the dynamical equation governing the behavior of the scalar form factor, $X_0(q)$. Our starting point is the Fig. 4, where we have the diagrammatic representation of the quark-ghost scattering kernel, $H^{[1]}$, at the "one-loop dressed" level. In this approximation $H^{[1]}$ is given by

$$H^{[1]} = Z_H - i\frac{g^2 C_A}{2} \int_k D(q-k) G_v \Delta^{\mu\nu}(k) S(k+p_2) \Gamma_\mu(p_2, -p_2 - k, k)\,. \tag{14}$$

To evaluate Eq. (14) further, we will use the tree-level expression for the gluon-ghost vertex $G_\nu = (q-k)_\nu$, whereas for the vertex Γ_μ we employ the following simpler Ansatz

$$\Gamma_\mu(p_2, -k - p_2, k) = F(k)X_0(k)\Gamma'_\mu(p_2, -k - p_2, k)\,, \tag{15}$$

with

$$\begin{aligned} \Gamma'_\mu(p_2, -k - p_2, k) \quad &= \frac{1}{2}\left[A(p_2 + k) + A(p_2)\right]\gamma_\mu \\ &+ \frac{1}{2}\frac{k^\mu}{k^2}\Big[\left[A(p_2 + k) - A(p_2)\right](2\not{p}_2 + \not{k}) - 2\left[B(p_2 + k) - B(p_2)\right]\Big]\,. \end{aligned} \tag{16}$$

Notice that the quark-gluon vertex given in Eq. (15) satisfies the STI of Eq. (4).

In this work we restrict ourself to the study of X_0 in the so-called *quark symmetric limit*, where the quark momenta have the same magnitude and opposite signs, *i.e.* $p_1 = -p/2$, $p_2 = p/2$

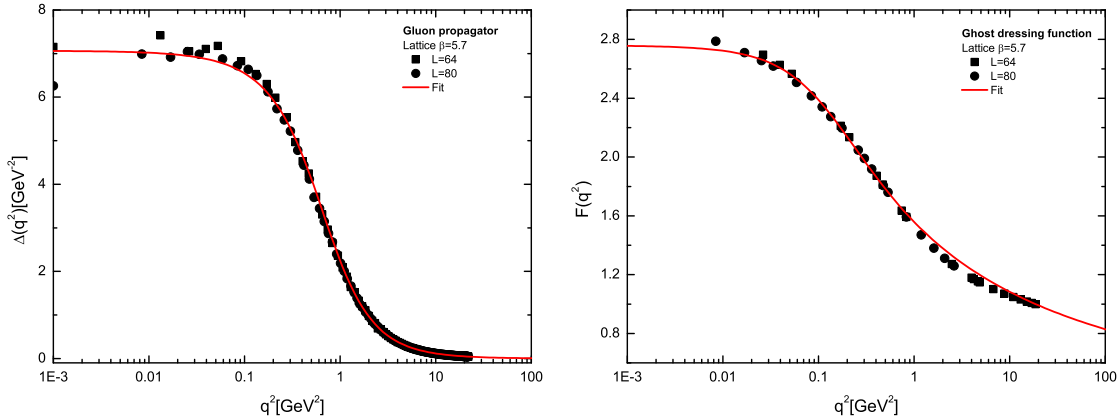

Figure 5. Lattice data (black dots) for the gluon propagator, $\Delta(q)$, (left panel) and the ghost dressing function, $F(q)$ (right panel) renormalized at $\mu = 4.3$ GeV [12]. The red continuous curve are the fits for the lattice data.

and $q = -p$ [6]. Taking the appropriate traces in Eq. (6), it is straightforward to derive from Eq. (14) the following linear integral equation for the form factor $X_0^{[1]}$ (in the Euclidean space)

$$X_0^{[1]}(p) \;=\; Z_H + \frac{g^2 C_A}{8}\int_k \frac{D(p+k)F(k)\Delta(k)A_2[A_2+A_1]}{A_2^2(p/2+k)^2+B_2^2}\left[p^2 - \frac{(p\cdot k)^2}{k^2}\right] X_0^{[1]}(k)\,. \quad (17)$$

where we have introduced the shorthand notation $A_1 = A(p/2)$, $A_2 = A(p/2+k)$, $B_1 = B(p/2)$, and $B_2 = B(p/2+k)$.

4. Numerical analysis

We clearly see that the coupled system for $A(p)$ and $B(p)$ given by Eq. (13) depends on the nonperturbative form of the three basic Greens functions, namely $\Delta(q)$, $F(q)$ and $X_0^{[1]}(p)$. For $\Delta(q)$ and $F(q)$ we use the lattice data obtained in Ref. [12], and shown in the Fig. 5. We clearly see that both lattice results for $\Delta(q)$, $F(q)$ are infrared finite. Such a feature can be associated to a purely non-perturbative effect that gives rise to a dynamical gluon mass [16, 17], which saturates the gluon propagator in the infrared.

Now, we are in position to solve the system formed by Eqs. (13) and (17). Substituting into Eqs. (13) the lattice data for $\Delta(q)$ and $F(q)$, with the modification $Z_c^{-1}\mathcal{K}_{A,B} \to \mathcal{K}_{A,B}\,F(q)$, to enforce the correct renormalization group behavior of the dynamical mass (see discussion in [6].), we determine numerically the unknown functions $A(p)$, $B(p)$ and $X_0^{[1]}(p)$ when $\alpha(\mu) = 0.29$ for $\mu = 4.3$ GeV.

The result for $X_0^{[1]}(p)$ is shown in Fig. 6. Notice that we have fixed the value of Z_H, appearing in Eq. (17), by enforcing that the renormalization condition, $X_0^{[1]}(\mu) = 1$.

On the left panel of Fig. 6, we present the case where $m_0 = 5$ MeV. As happened in the analysis presented in Ref. [6], $X_0^{[1]}(p)$ displays a maximum located 1 GeV, while in the ultraviolet and infrared regions $X_0^{[1]}(p) \to 1$ (black curve). Notice that the resulting peak is slightly higher than the one obtained by simply substituting $X_0^{[1]}(k) = 1$ on the rhs of (17) (green dashed curve) [6]. On the right panel, we show the behavior of $X_0^{[1]}(p)$ for the following current masses:

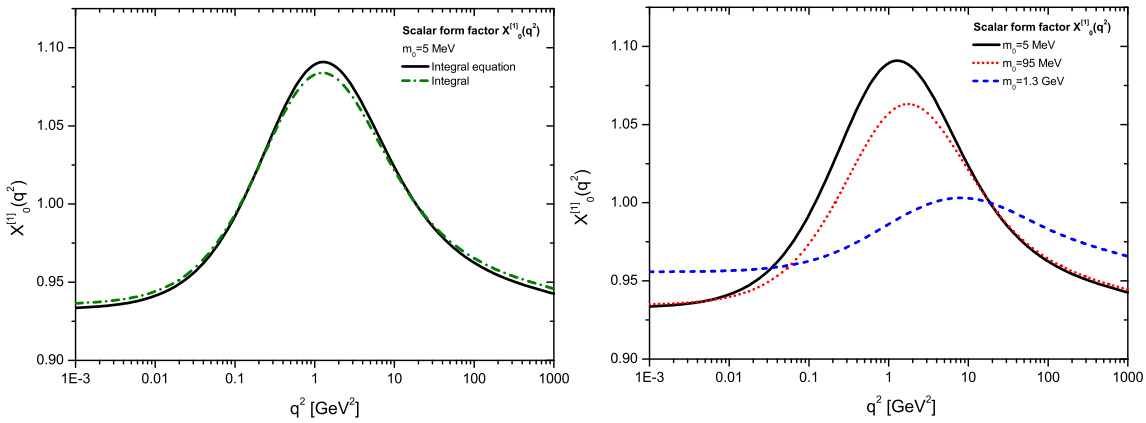

Figure 6. The numerical result for the form factor $X_0^{[1]}(q)$ given by Eq. (17).

$m_0 = 5$ MeV (black continuous), $m_0 = 95$ MeV (red dotted) and $m_0 = 1.3$ GeV (blue dashed). We clearly see a suppression as the current mass increases. Although this peak is not very pronounced, it turns out to be essential for providing to the kernel of the gap equation the enhancement required for the generation of phenomenologically compatible constituent quark masses.

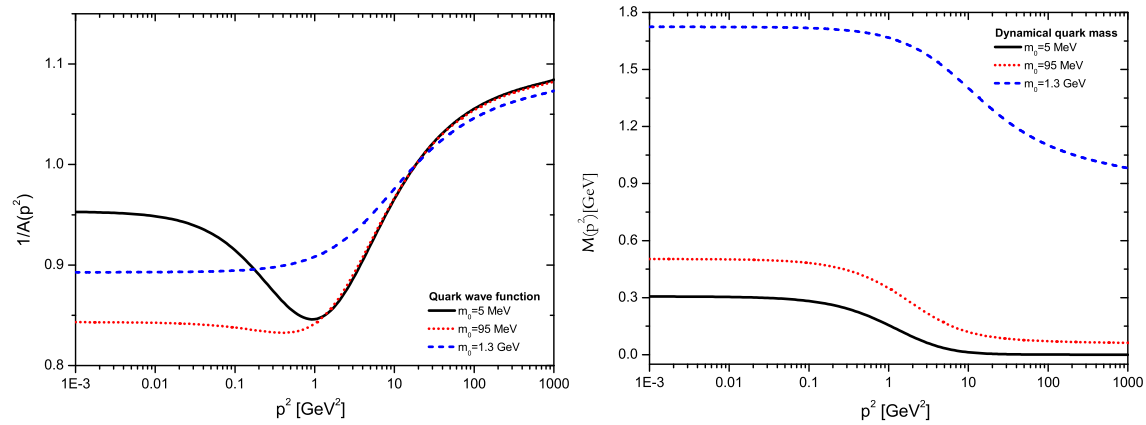

Figure 7. The numerical solution for the quark wave function $A^{-1}(p)$ (left panel). Dynamical quark mass $\mathcal{M}(p)$ (right panel).

Finally, in Fig. 7 we show the corresponding results for the quark wave function $A^{-1}(p)$ (left panel) and for the dynamical quark mass $\mathcal{M}(p)$ (right panel). From this plot one observes the effects due to the inclusion of a current mass term, which explicitly breaks the chiral symmetry. We present the results for three different current quark masses $m_0 = 5$ MeV (black continuous), $m_0 = 95$ MeV (red dotted) and $m_0 = 1.3$ GeV (blue dashed), corresponding to the up/down, strange and charm quarks. It is clear that the amount of dynamical mass generated in the case of light quarks is much more considerable than for the heavier ones. For example, for $m_0 = 5$ MeV, the dynamical mass produced is $\mathcal{M}(0) = 310$ MeV, for $m_0 = 95$ MeV we

obtain $\mathcal{M}(0) = 503$ MeV, whereas for $m_0 = 1.3$ MeV we obtain $\mathcal{M}(0) = 1.72$ GeV. In addition, using the Pagels-Stokar formula [18], we have computed the pion decay constant for the case of $m_0 = 5$ MeV. The result obtained is 98.4 MeV, which is in good agreement with the experiment value of 93 MeV [19].

5. Conclusions

It has been shown that the quark gap equation gives rise to phenomenologically compatible results for the dynamical quark mass using an infrared finite gluon propagator. The crucial ingredient in this analysis is the structure of the non-abelian quark-gluon vertex and the quark-ghost scattering kernel. Both quantities are responsible for furnishing the additional strength in the intermediate region around 1 GeV, necessary for the breaking of the CS. In addition, light quarks are significantly more affected by the dynamical mass generation than the heavier ones.

Acknowledgments

The authors thank the organizers of the XIII International Workshop on Hadron Physics for their hospitality. This work was developed under the support of the National Council for Scientific and Technological Development-CNPq (JCC and ACA) and São Paulo Research Foundation - FAPESP (ACA).

References

[1] C. D. Roberts and A. G. Williams, Prog. Part. Nucl. Phys. **33**, 477 (1994).
[2] J. Papavassiliou, J. Phys. Conf. Ser. **631**, no. 1, 012006 (2015).
[3] I. C. Cloet and C. D. Roberts, Prog. Part. Nucl. Phys. **77**, 1 (2014).
[4] C. D. Roberts, arXiv:1509.02925 [nucl-th].
[5] J. Papavassiliou and J. M. Cornwall, Phys. Rev. D **44**, 1285 (1991).
[6] A. C. Aguilar and J. Papavassiliou, Phys. Rev. D **83**, 014013 (2011).
[7] C. S. Fischer and R. Alkofer, Phys. Rev. D **67**, 094020 (2003).
[8] A. C. Aguilar, D. Binosi, D. Ibañez and J. Papavassiliou, Phys. Rev. D **90**, no. 6, 065027 (2014).
[9] A. C. Aguilar, D. Binosi, J. C. Cardona and J. Papavassiliou, PoS ConfinementX , 103 (2012).
[10] A. Cucchieri and T. Mendes, PoS **LAT2007**, 297 (2007).
[11] A. Cucchieri and T. Mendes, Phys. Rev. D **81**, 016005 (2010).
[12] I. L. Bogolubsky, E. M. Ilgenfritz, M. Muller-Preussker and A. Sternbeck, PoS LAT **2007**, 290 (2007).
[13] W. J. Marciano and H. Pagels, Phys. Rept. **36**, 137 (1978).
[14] A. I. Davydychev, P. Osland and L. Saks, Phys. Rev. D **63**, 014022 (2001).
[15] J. S. Ball and T. W. Chiu, Phys. Rev. D **22**, 2542 (1980).
[16] A. C. Aguilar, D. Binosi and J. Papavassiliou, Phys. Rev. D **78**, 025010 (2008).
[17] A. C. Aguilar, D. Binosi and J. Papavassiliou, JHEP **1201**, 050 (2012).
[18] H. Pagels and S. Stokar, Phys. Rev. D **20**, 2947 (1979).
[19] K. A. Olive *et al.* [Particle Data Group Collaboration], Chin. Phys. C **38**, 090001 (2014).